View metadata, citation and similar papers at core.ac.uk

brought to you by CORE

provided by IntechOpen

We are IntechOpen, the world's leading publisher of Open Access books Built by scientists, for scientists

4,800
Open access books available

122,000
International authors and editors

135M
Downloads

Our authors are among the

154
Countries delivered to

TOP 1%
most cited scientists

12.2%
Contributors from top 500 universities

CLARIVATE ANALYTICS BOOK CITATION INDEX INDEXED

WEB OF SCIENCE™

Selection of our books indexed in the Book Citation Index in Web of Science™ Core Collection (BKCI)

Interested in publishing with us?
Contact book.department@intechopen.com

Numbers displayed above are based on latest data collected.
For more information visit www.intechopen.com

1

Mathematical Models of Heat Flow in Edge-Emitting Semiconductor Lasers

Michał Szymański
Institute of Electron Technology
Poland

1. Introduction

Edge-emitting lasers started the era of semiconductor lasers and have existed up to nowadays, appearing as devices fabricated out of various materials, formed sometimes in very tricky ways to enhance light generation. However, in all cases radiative processes are accompanied by undesired heat-generating processes, like non-radiative recombination, Auger recombination, Joule effect or surface recombination. Even for highly efficient laser sources, great amount of energy supplied by pumping current is converted into heat.

High temperature leads to deterioration of the main laser parameters, like threshold current, output power, spectral characteristics or lifetime. In some cases, it may result in irreversible destruction of the device via catastrophic optical damage (COD) of the mirrors. Therefore, deep insight into thermal effects is required while designing the improved devices.

From the thermal point of view, the laser chip (of dimensions of 1-2 mm or less) is a rectangular stack of layers of different thickness and thermal properties. This stack is fixed to a slightly larger heat spreader, which, in turn, is fixed to the huge heat-sink (of dimensions of several cm), transferring heat to air by convection or cooled by liquid or Peltier cooler. Schematic view of the assembly is shown in Fig. 1. Complexity and large size differences between the elements often induce such simplifications like reduction of the dimensionality of equations, thermal scheme geometry modifications or using non-uniform mesh in numerical calculations.

Mathematical models of heat flow in edge-emitting lasers are based on the heat conduction equation. In most cases, solving this equation provides a satisfactory picture of thermal behaviour of the device. More precise approaches use in addition the carrier diffusion equation. The most sophisticated thermal models take into consideration variable photon density found by solving photon rate equations.

The heat generated inside the chip is mainly removed by conduction and, in a minor degree, by convection. Radiation can be neglected. Typical boundary conditions for heat conduction equation are the following: isothermal condition at the bottom of the device, thermally insulated side walls, convectively cooled upper surface. It must be said that obtaining reliable temperature profiles is often impossible due to individual features of particular devices, which are difficult to evaluate within the quantitative analysis. Mounting imperfections

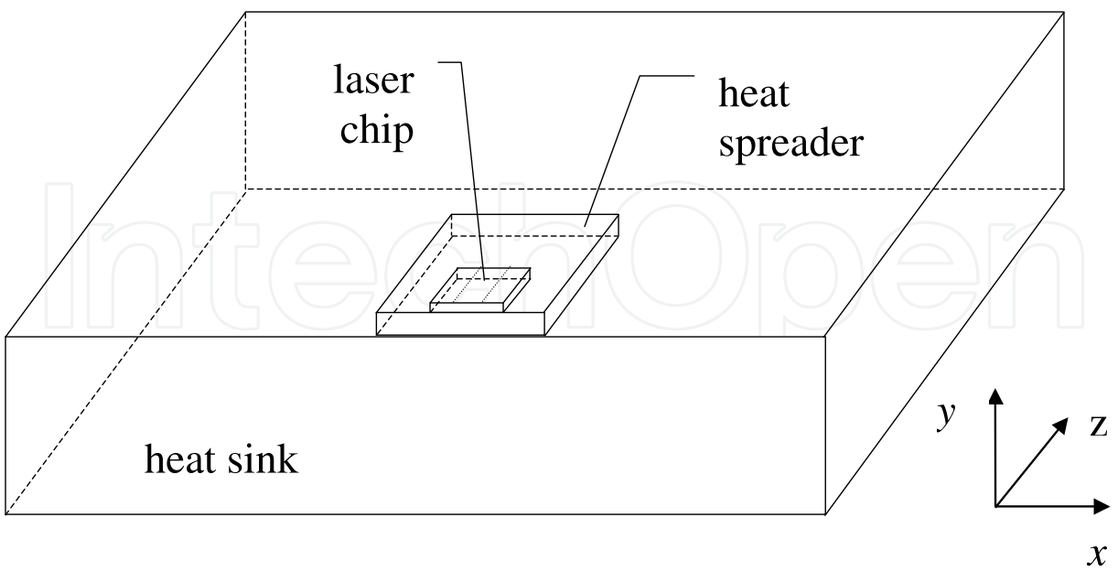

Fig. 1. Schematic view of the laser chip or laser array mounted on the heat spreader and heat sink (not in scale).

like voids in the solder or overhang (the chip does not adhere to the heat-spreader entirely) may significantly obstruct the heat transfer. Surface recombination, the main mirror heating mechanism in bipolar devices, strongly depends on facet passivation.

Since quantum cascade lasers (QCL's) exploit superlattices (SL's) as active layers, they have brought new challenges in the field of thermal modelling. Numerous experiments show that the thermal conductivity of a superlattice is significantly reduced. The phenomenon can be explained in terms of phonon transport across a stratified medium. As a consequence, mathematical models of heat flow in quantum cascade lasers resemble those created for standard edge-emitting lasers, but the stratified active region is replaced by an equivalent layer described by anisotropic thermal conductivity. In earlier works, the cross-plane and in-plane values of this parameter were obtained by arbitrary reduction of bulk values or treated as fitting parameters. Recently, some theoretical methods of assessing the thermal conductivity of superlattices have been developed.

The present chapter is organised as follows. In sections 2, 3 and 4, one can find the description of static thermal models from the simplest to the most complicated ones. Section 5 provides a discussion of the non-standard boundary condition assumed at the upper surface. Dynamical issues of thermal modelling are addressed in section 6, while section 7 is devoted to quantum cascade lasers. In greater part, the chapter is a review based on the author's research supported by many other works. However, Fig. 7, 8, 12 and 13 present the unpublished results dealing with facet temperature reduction techniques and dynamical thermal behaviour of laser arrays. Note that section 8 is not only a short revision of the text, but contains some additional information or considerations, which may be useful for thermal modelling of edge-emitting lasers. The most important mathematical symbols are presented in Table 1. Symbols of minor importance are described in the text just below the equations, in which they appear.

Symbol	Description
A_{nr}	non-radiative recombination coefficient
B	bi-molecular recombination coefficient
b	chip width (see Fig. 2)
C_A	Auger recombination coefficient
c_h	specific heat
D	diffusion coefficient
d_n	total thickness of the n-th medium
g	heat source function
I	driving current
L	resonator length
n_{eff}	effective refractive index
n_i	number of interfaces
N, N_{tr}	carrier concentration, transparency carrier concentration
R_f, R_b	power reflectivity of the front and back mirror
$r_{\mathrm{Bd}}(1 \to 2)$	TBR for the heat flow from medium 1 to 2
S	total photon density
S_f, S_b	photon density of the forward and backward travelling wave
S_{av}	averaged photon density
t	time
T	temperature
T_{up}	temperature of the upper surface
V	voltage
v_{sur}	surface recombination velocity
w	contact width (see Fig. 2)
y_t	top of the structure (see Fig. 2)
x, y, z	spatial coordinates (see Fig. 1)
α	convection coefficient
α_{gain}	linear gain coefficient
α_{int}	internal loss within the active region
β	spontaneous emission coupling coefficient
Γ	confinement factor
λ	thermal conductivity
$\lambda_\perp$,$\lambda_\parallel$	thermal conductivity of QCL's active layer in the direction perpendicular and parallel to epitaxial layers, respectively
ν	frequency
ρ_n	density, subscript n (if added) denotes the medium number
τ, τ_{av}	carrier lifetime, averaged carrier lifetime
c, e, h, k_B	physical constants: light velocity, elementary charge, Planck and Boltzmann constants, respectively.

Table 1. List of symbols.

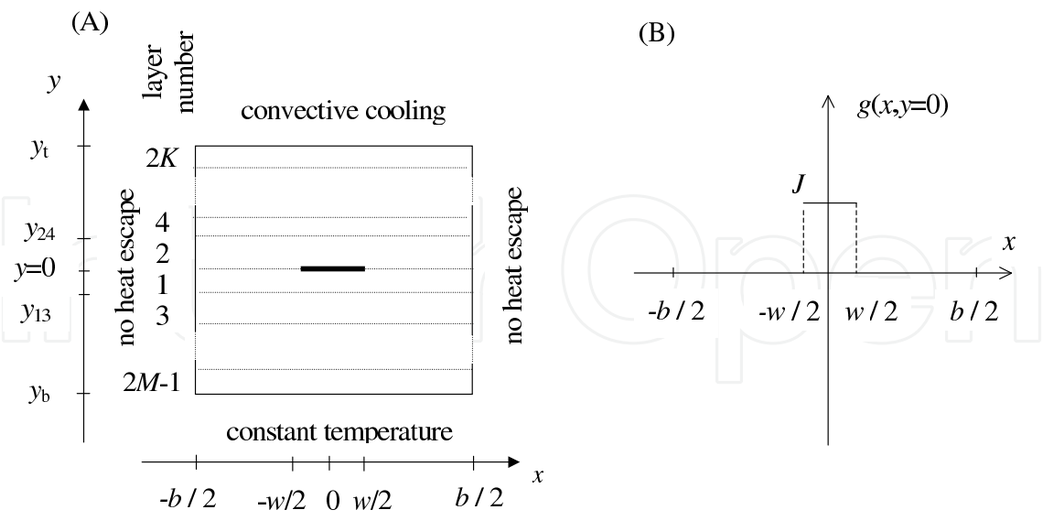

Fig. 2. Schematic view of a laser chip cross-section (A). Function describing the heat source (B).

2. Models based on the heat conduction equation only

Basic thermal behaviour of an edge-emitting laser can be described by the stationary heat conduction equation:

$$\nabla(\lambda(y)\nabla T(x,y)) = -g(x,y) \tag{1}$$

accepting the following assumptions (see Fig. 2):

— the laser is a rectangular stack of layers of different thickness and thermal conductivities; [1]

— there is no heat escape from the top and side walls, while the temperature of the bottom of the structure is constant;

— the active layer is the only heat source in the structure and it is represented by infinitely thin stripe placed between the waveguide layers.

The heat power density is determined according to the crude approximation:

$$g(x,y) = \frac{VI - P_{out}}{Lw}, \tag{2}$$

which physically means that the difference between the total power supplied to the device and the output power is uniformly distributed over the surface of the selected region.[2] The problem was solved analytically by Joyce & Dixon (1975). Further works using this model introduced convective cooling at the top of the laser, considered extension and diversity of heat sources or changed the thermal scheme in order to take into account the non-ideal heat sink (Bärwolff et al. (1995); Puchert et al. (1997); Szymański et al. (2007; 2004)). Such approach allows to calculate temperature inside the resonator, while the temperature in the vicinity of

[1] Note that the thermal scheme can be easily generalised to laser array by periodic duplication of stack along the x axis.

[2] In a three-dimensional case the surface is replaced by the volume.

mirrors is reliable only in the near-threshold regime. The work by Szymański et al. (2007) can be regarded as a recent version of this model and will be briefly described below.
Assuming no heat escape from the side walls:

$$\frac{\partial}{\partial x}T(\pm\frac{b}{2},y)=0 \tag{3}$$

and using the separation of variables approach (Bärwolff et al. (1995); Joyce & Dixon (1975)), one obtains the solution for T in two-fold form. In the layers above the active layer (n - even) temperature is described by

$$T_n(x,y)=A_{2K}^{(0)}(w_{A,n}^{(0)}+w_{B,n}^{(0)}y)+ \sum_{k=1}^{\infty}A_{2K}^{(k)}[w_{A,n}^{(k)}exp(\mu_k y)+w_{B,n}^{(k)}exp(-\mu_k y)]cos(\mu_k x), \tag{4}$$

while under the active layer (n - odd) it takes the form:

$$T_n(x,y)=A_{2M-1}^{(0)}(w_{A,n}^{(0)}+w_{B,n}^{(0)}y)+ \sum_{k=1}^{\infty}A_{2M-1}^{(k)}[w_{A,n}^{(k)}exp(\mu_k y)+w_{B,n}^{(k)}exp(-\mu_k y)]cos(\mu_k x). \tag{5}$$

In (4) and (5) $\mu_k=2k\pi/b$ is the separation constant and thus it appears in both directions (x and y). Integer number k numerates the heat modes. Coefficients $w_{A,n}^{(k)}$ and $w_{B,n}^{(k)}$ and relation between $A_{2K}^{(k)}$ and $A_{2M-1}^{(k)}$ can be found in Szymański (2007). They are determined by the bottom boundary condition, continuity conditions for the temperature and heat flux at the layer interfaces and the top boundary condition.

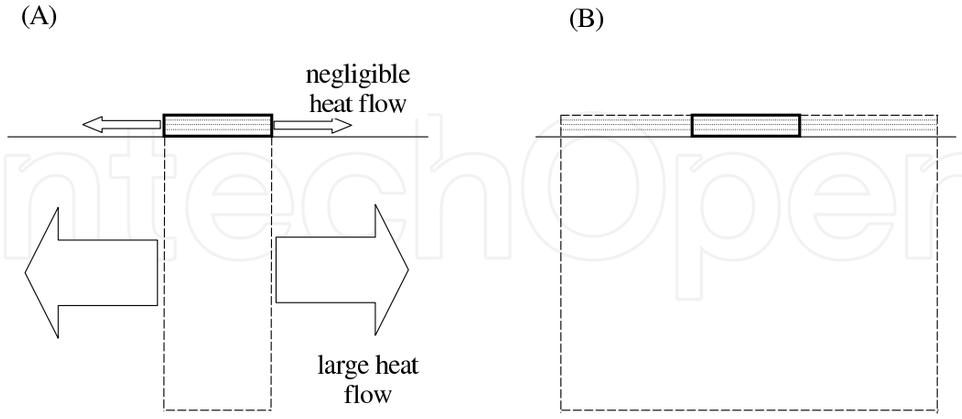

Fig. 3. Thermal scheme modification. Assuming larger b allows to keep the rectangular cross-section of the whole assembly and hence equations (4) and (5) can be used.

The results obtained according to the model described above are presented in Table 2. The calculated values are slightly underestimated due to bonding imperfections, which elude

Device number	Heterostructure A	Heterostructure B	Heterostructure C
1	12.03/7.38	11.23/7.31	8.9/8.24
2	13.35/7.38	12.17/7.31	7.0/4.76

Table 2. Measured/calculated thermal resistances in K/W (Szymański et al. (2007)).

qualitative assessment. A similar problem was described in Manning (1981), where even greater discrepancies between theory and experiment were obtained. For the properly mounted device C1 excellent convergence is found.
Improving the accuracy of calculations was possible due to taking into account the finite thermal conductivity of the heat sink material by thermal scheme modifications (see Fig. 3). Assuming constant temperature at the chip-heat spreader interface leads to significant errors, especially for p-side-down mounting (see Fig. 4).
The analytical approach presented above has been described in detail since it has been developed by the author of this chapter. However, it should not be treated as a favoured one. In recent years, numerical methods seem to prevail. Pioneering works using Finite Element Method (FEM) in the context of thermal investigations of edge-emitting lasers have been described by Sarzała & Nakwaski (1990; 1994). Broader discussion of analytical vs. numerical methods is presented in 8.3.

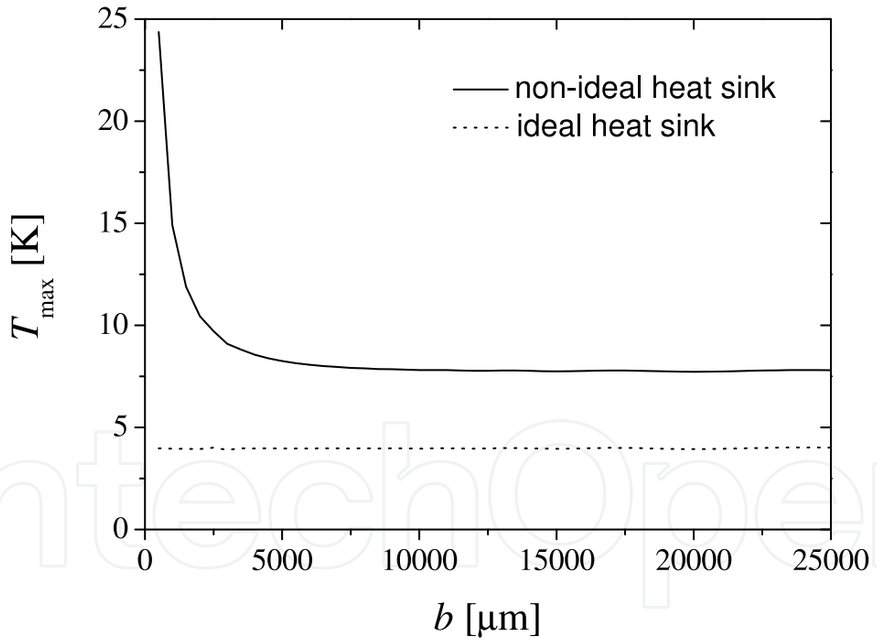

Fig. 4. Maximum temperature inside the laser for *p*-side down mounting. It is clear that the assumption of ideal heat sink leads to a 50% error in calculations (Szymański et al. (2007)).

Thermal effects in the vicinity of the laser mirror are important because of possible COD during high-power operation. Unfortunately, theoretical investigations of these processes, using the heat conduction only, is rather difficult. There are two main mirror heating mechanisms (see Rinner et al. (2003)): surface recombination and optical absorption. Without including additional equations, like those described in sections 3 and 4, assessing the heat

source functions may be problematic. An interesting theoretical approach dealing with mirror heating and based on the heat conduction only, can be found in Nakwaski (1985; 1990). However, both works consider the time-dependent picture, so they will be mentioned in section 6.

3. Models including the diffusion equation

Generation of heat in a semiconductor laser occurs due to: (A) non-radiative recombination, (B) Auger recombination, (C) Joule effect, (D) spontaneous radiative transfer, (E) optical absorption and (F) surface recombination. The effects (A)—(C) and (E,F) are discussed in standard textbooks (see Diehl (2000) or Piprek (2003)). Additional interesting information about mirror heating mechanisms (E,F) can be found in Rinner et al. (2003). The effect (D) will be briefly described below.

Apart from stimulated radiation, the laser active layer is a source of spontaneous radiation. The photons emitted in this way propagate isotropically in all directions. They penetrate the wide-gap layers and are absorbed in narrow-gap layers (cap or substrate) creating the additional heat sources (see Nakwaski (1979)). Temperature calculations by Nakwaski (1983a) showed that the considered effect is comparable to Joule heating in the near-threshold regime. On the other hand, it is known that below the threshold spontaneous emission grows with pumping current and saturates above the threshold. Thus, the radiative transfer may be recognised as a minor effect and will be neglected in calculations presented in this chapter.

Note that processes (A)—(C) and (F) involve carriers, so $g(x,y,z)$ should be a carrier dependent function. To avoid crude estimations, like equation (2), a method of getting to know the carrier distribution in regions essential for thermal analysis is required.

3.1 Carrier distribution in the laser active layer

An edge-emitting laser is a p-i-n diode operating under forward bias and in the plane of junction the electric field is negligible. Therefore, the movement of the carriers is governed by diffusion. Bimolecular recombination and Auger process engage two and three carriers, respectively. Such quantities like pumping or photon density are spatially inhomogeneous. Far from the pumped region, the carrier concentration falls down to zero level. At the mirrors, surface recombination occurs. Taking all these facts into account, one concludes that carrier concentration in the active layer can be described by a nonlinear diffusion equation with variable coefficients and mixed boundary conditions. Solving such an equation is really difficult, but the problem can often be simplified to 1-dimensional cases. For example, if problems of beam quality (divergence or filamentation) are discussed, considering the lateral direction only is a good enough approach. In the case of a thermal problem, since surface recombination is believed to be a very efficient facet heating mechanism responsible for COD, considering the axial direction is required and the most useful form of the diffusion equation can be written as

$$D\frac{d^2N}{dz^2} - \frac{c}{n_{eff}}\Gamma G(N)S(z) - \frac{N}{\tau} + \frac{I}{eV} = 0, \tag{6}$$

where linear gain $G(N) = \alpha_{gain}(N - N_{tr})$ and non-linear carrier lifetime $\tau(N) = (A_{nr} + BN + C_A N^2)^{-1}$ have been assumed. The surface recombination at the laser facets is

expressed through the boundary conditions:

$$D\frac{dN(0)}{dz} = v_{sur}N(0), \qquad D\frac{dN(L)}{dz} = -v_{sur}N(L). \tag{7}$$

The problem of axial carrier concentration in the active layer of an edge-emitting laser was investigated by Szymański (2010). Three cases were considered:

(i) the nonlinear diffusion equation with variable coefficients (equation (6) and boundary conditions (7)) ;

(ii) the linear diffusion equation with constant coefficients derived form equation (6) by assuming the averaged carrier lifetime τ_{av} and averaged photon density S_{av};

(iii) the algebraic equation derived form equation (6) by neglecting the diffusion ($D = 0$).

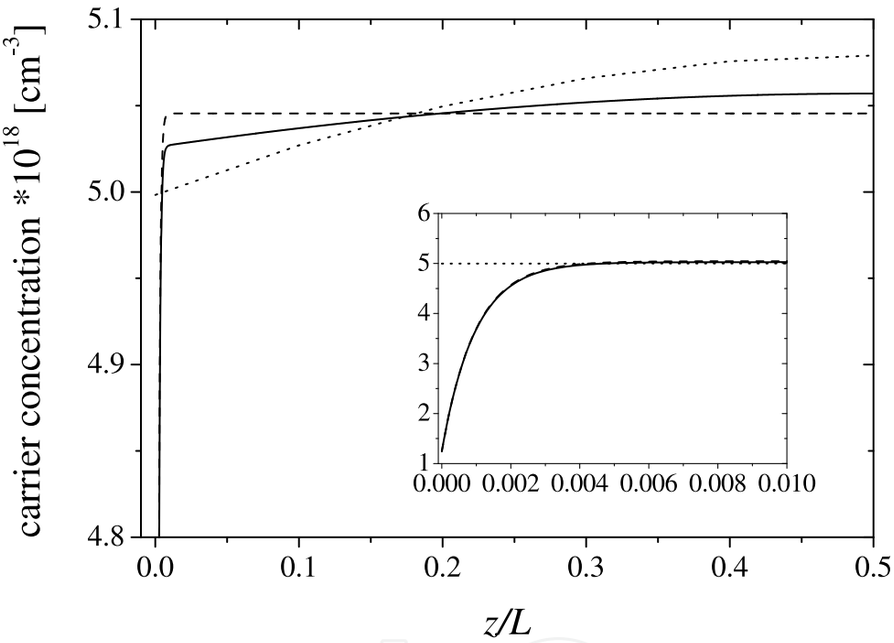

Fig. 5. Axial (mirror to mirror) carrier concentration in the active layer calculated according to algebraic equation (dotted line), linear diffusion equation with constant coefficients (dashed line) and nonlinear diffusion equation with variable coefficients (solid line) (Szymański (2010)).

The results are shown in Fig. 5. It is clear that the approach (iii) yields a crude estimation of the carrier concentration in the active layer. However, for thermal modelling, where phenomena in the vicinity of facets are crucial due to possible COD processes, the diffusion equation must be solved. In many works (see for example Chen & Tien (1993), Schatz & Bethea (1994), Mukherjee & McInerney (2007)), the approach (ii) is used. It seems to be a good approximation for a typical edge-emitting laser, which is an almost axially homogeneous device in the sense that the depression of the photon density does not vary too much or temperature differences along the resonator are not so significant to dramatically change the

non-linear recombination terms B and C_A. The approach (i) is useful in all the cases where the above-mentioned axial homogeneity is perturbed. In particular, the approach is suitable for edge-emitting lasers with modified regions close to facets. These modifications are meant to achieve mirror temperature reduction through placing current blocking layers (Rinner et al. (2003)), producing non-injected facets (so called NIFs) (Pierscińska et al. (2007)) or generating larger band gaps (Watanabe et al. (1995)).

3.2 Carrier-dependent heat source function

The knowledge of axial carrier concentration opens up the possibility to write the heat source function more precisely compared to equation (2), namely

$$g(x,y,z) = g_a(x,y,z) + g_J(x,y,z), \tag{8}$$

where the first term describes the heat generation in the active layer and the second - Joule heating. According to Romo et al. (2003):

$$g_a(x,y,z) = [(A_{nr} + C_A N^2(z))N(z) + \frac{c}{n_{eff}}\alpha_{int}S_{av} + \frac{\mu_{sur}N(z=0)}{d_{sur}}\Pi_{sur}(z)]h\nu\Pi_a(x,y,z). \tag{9}$$

The terms in the right hand side of equation (9) are related to non-radiative recombination, Auger processes, absorption of laser radiation and surface recombination at the facets, respectively. Assessing the value of S_{av} was widely discussed by Szymański (2010). The Π's are positioning functions:

$$\Pi_{sur}(z) = \begin{cases} 1, & \text{for } 0 < z < d_{sur}; \\ 0, & \text{for } z > d_{sur}, \end{cases} \tag{10}$$

expresses the assumption that the defects in the vicinity of the facets are uniformly distributed within a distance $d_{sur} = 0.5\mu m$ from the facet surface (Nakwaski (1990); Romo et al. (2003)), while $\Pi_a(x,y,z) = 1$ for x,y,z within the active layer and $\Pi_a(x,y,z) = 0$ elsewhere.
The effect of Joule heating is strictly related to the electrical resistance of a particular layer. High values of this parameter are found in waveguide layers, substrate and p-doped cladding due to the lack of doping, large thickness and low mobility of holes, respectively Szymański et al. (2004). Thus, it is reasonable to calculate the total Joule heat and assume that it is uniformly generated in layers mentioned above of total volume V_{hr}:

$$g_J(x,y,z) = \frac{I^2 R_s}{V_{hr}}, \tag{11}$$

where R_s is the device series resistance.

3.3 Selected results

Axial (mirror to mirror) distribution of relative temperature[3] in the active layer of the edge-emitting laser is shown in Fig. 6. It has been calculated numerically solving the

[3] The temperature exceeding the ambient temperature.

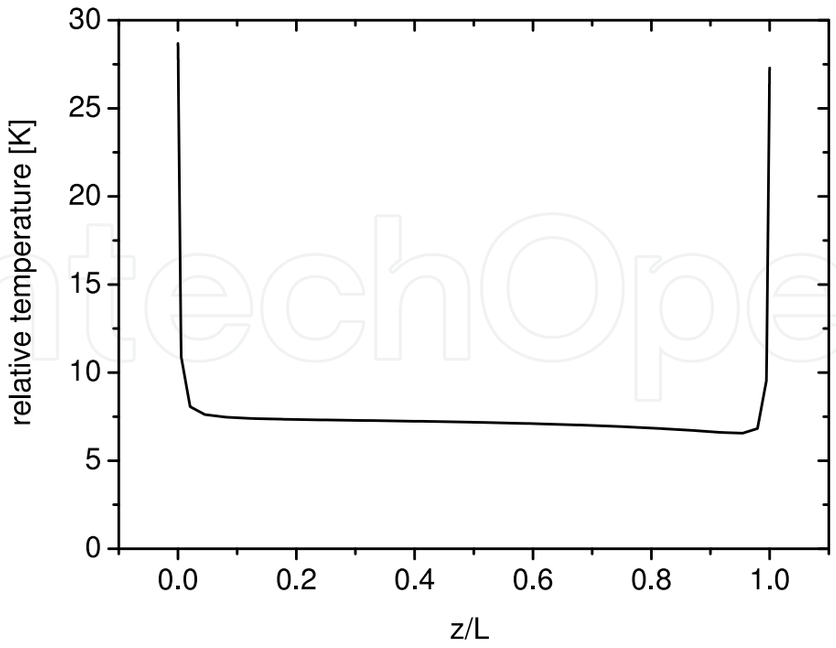

Fig. 6. Axial (mirror to mirror) distribution of relative temperature in the active layer.

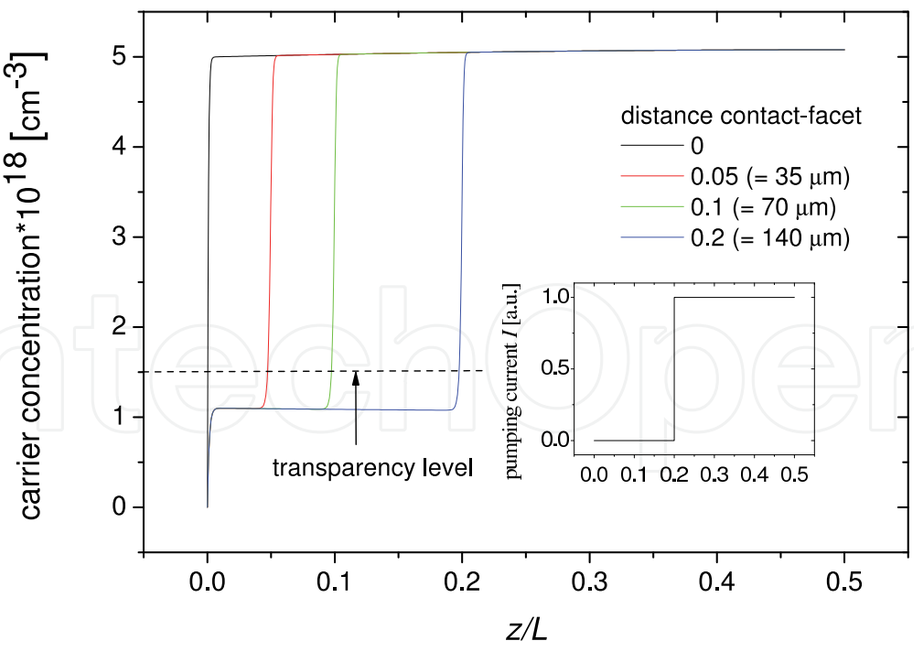

Fig. 7. Axial distribution of carriers in the active layer for the laser with non-injected facets. The inset shows the step-like pumping profile.

three-dimensional heat conduction equation.[4] Heat source has been inserted according to (8)-(11), where $N(z)$ has been calculated analytically from the linear diffusion equation with constant coefficients (approach (ii) from section 3.1). Fig. 6 is in qualitative agreement with plots presented by Chen & Tien (1993); Mukherjee & McInerney (2007); Romo et al. (2003), where similar or more advanced models were used. Note that the temperature along the resonator axis is almost constant, while it rises rapidly in the vicinity of the facets. The small asymmetry is caused by the location of the laser chip: the front facet is over the edge of the heat sink, so the heat removal is obstructed.

Facet temperature reduction techniques are often based on the idea of suppressing the surface recombination by preventing the current flow in the vicinity of facets. It can be realised by placing current blocking layers (Rinner et al. (2003)) or producing non-injected facets (so called NIFs) (Pierscińska et al. (2007)). To investigate such devices the author has solved the equation (6) numerically[5] inserting step-like function $I(z)$. Fig. 7 shows that, in the non-injected region, the carrier concentration rapidly decreases to values lower than transparency level, which is an undesired effect and may disturb laser operation. A solution to this problem, although technologically difficult, can be producing a device with segmented contact. Even weak pumping near the mirror drastically reduces the length of the non-transparent region, which is illustrated in Fig. 8.

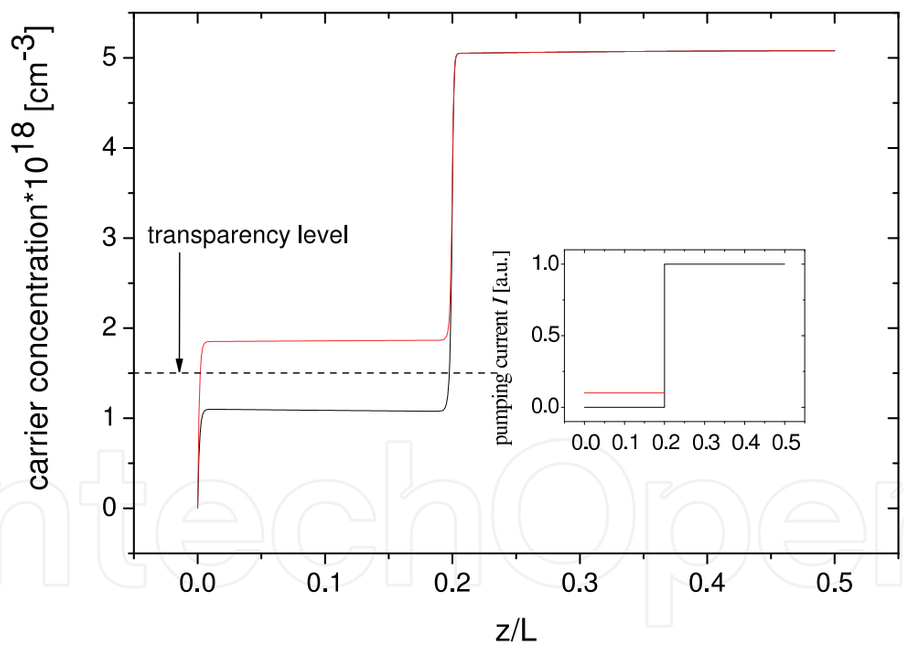

Fig. 8. Axial distribution of carriers in the active layer for the laser with non- and weakly-pumped near-facet region. The inset shows the pumping profile for both cases.

[4] Calculations have been done by Zenon Gniazdowski using the commercial software CFDRC (http://www.cfdrc.com/).

[5] The commercial software FlexPDE (http://www.pdesolutions.com/) has been used.

4. Models including the diffusion equation and photon rate equations

The most advanced thermal model is described by Romo et al. (2003). It takes into account electro-opto-thermal interactions and is based on 3-dimensional heat conduction equation

$$\nabla(\lambda(T)\nabla T) = -g(x,y,z,T), \tag{12}$$

1-dimensional diffusion equation (6), and photon rate equations

$$\frac{c}{n_{eff}}\frac{dS_f}{dz} = \frac{c}{n_{eff}}[\Gamma G(N,T) - \alpha_{int}]S_f + \beta B(T)N^2, \tag{13}$$

$$-\frac{c}{n_{eff}}\frac{dS_b}{dz} = \frac{c}{n_{eff}}[\Gamma G(N,T) - \alpha_{int}]S_b + \beta B(T)N^2. \tag{14}$$

The mirrors impose the following boundary conditions:

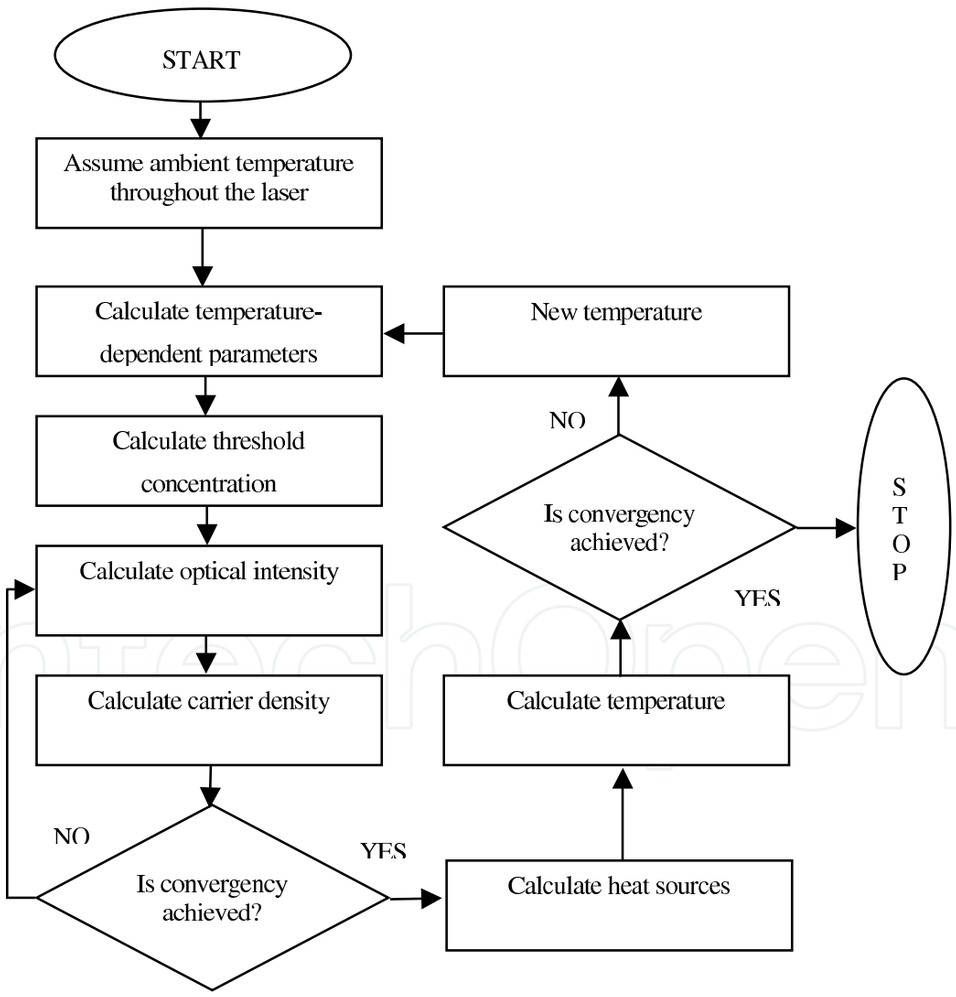

Fig. 9. Self-consistent algorithm (Romo et al. (2003)).

$$S_f(z=0) = R_f S_b(z=0),\ S_b(z=L) = R_b S_f(z=L). \tag{15}$$

Note the quadratic terms in equations (13) and (14), which describe the spontaneous radiation. To avoid problems with estimating the spatial distribution and extent of heat sources related to radiative transfer, Romo et al. (2003) have 'squeezed' the effect to the active layer. Such assumption resulted in inserting the term $(1-2\beta)B(T)N^2h\nu$ into equation (9).
The set of four differential equations mentioned above was solved numerically in the self-consistent loop, as schematically presented in Fig. 9. Several interesting conclusions formulated by Romo et al. (2003) are worth presenting here:

— the calculations confirmed that the temperature along the resonator axis is almost constant, while it rises rapidly in the vicinity of the facets (cf. Fig. 6);

— taking into account the non-linear temperature dependence of thermal conductivity significantly improves the accuracy of predicted temperature;

— using the 1-dimensional (axial direction) diffusion or photon rate equations is a good enough approach;

— heat conduction equation should be solved in 3 dimensions, reducing it to 2 dimensions is acceptable, while using the 1-dimensional form leads to significant overestimations of temperature in the vicinity of facets.

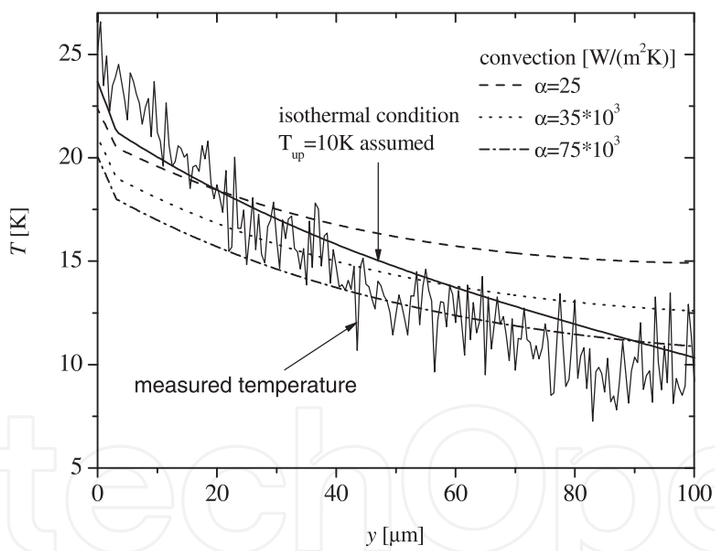

Fig. 10. Transverse temperature profiles across the substrate at $x = 0$ (Szymański (2007)).

5. Discussion of the upper boundary condition

Typical thermal models for edge-emitting lasers assume convectively cooled or thermally insulated (which is the case of zero convection coefficient) upper surface. In Szymański (2007), using the isothermal condition

$$T(x, y_t) = T_{up}. \tag{16}$$

instead of convection is proposed. The model is based on the solution of equation (1) obtained

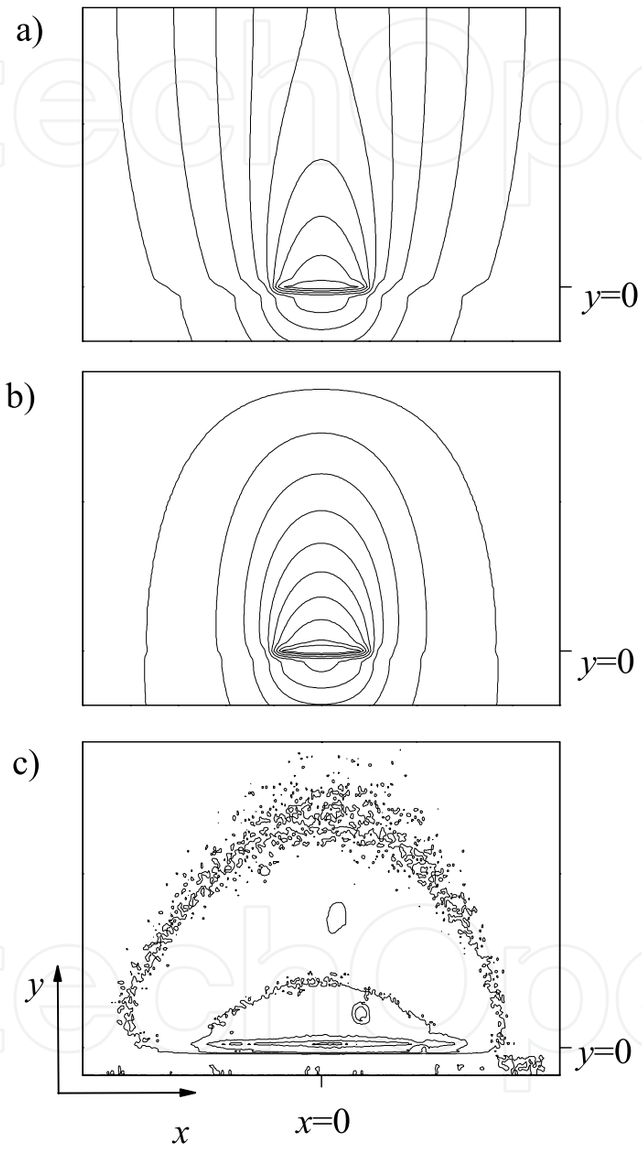

Fig. 11. Contour plot of temperature calculated under the assumption of convective cooling at the top surface (a), isothermal condition at the top surface (b) and measured by thermoreflectance method (c) (Szymański (2007)).

by separation-of-variables approach. Due to (16), the expression (4) describing temperature in the layers above the active layer must be modified in the following way:

$$T_n(x,y) = (\overline{w}^{(0)}_{A,n} A^{(0)}_{2K} + \overline{\overline{w}}^{(0)}_{A,n}) + (\overline{w}^{(0)}_{B,n} A^{(0)}_{2K} + \overline{\overline{w}}^{(0)}_{B,n}) y + \sum_{k=1}^{\infty} A^{(k)}_{2K} [w^{(k)}_{A,n} exp(\mu_k y) + w^{(k)}_{B,n} exp(-\mu_k y)] cos(\mu_k x). \quad (17)$$

Full analytical expressions can be found in Szymański (2007).
The investigations have been inspired by temperature maps obtained by thermoreflectance method (Bugajski et al. (2006); Wawer et al. (2005)) for *p*-down mounted devices. These maps suggest the presence of the region of constant temperature in the vicinity of the *n*-contact. Besides, the isothermal lines are rather elliptic, surrounding the hot active layer, than directed upward as calculated for convectively cooled surface. The results are presented in Fig. 10 and 11. It is clear that assuming the isothermal condition and convection at the top surface one gets nearly the same device thermal resistances, but with the first assumption closer convergence with thermoreflectance measurements is found.

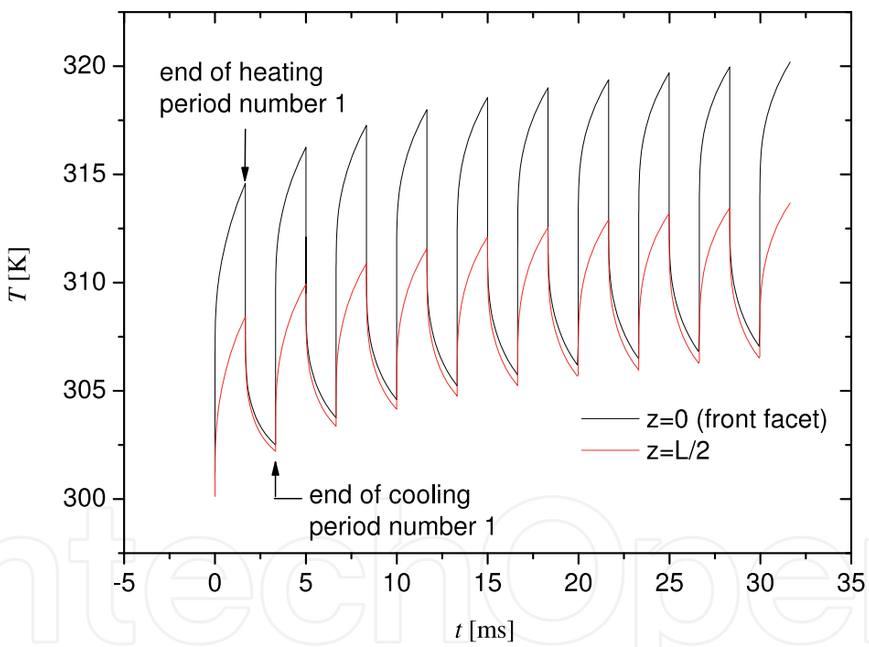

Fig. 12. Time evolution of central emitter active layer temperature.

6. Dynamical picture of thermal behaviour

Time-dependent models of edge-emitting lasers are considered rather seldom for two main reasons. First, edge-emitting lasers are predominantly designed for continuous-wave operation, so there is often no real need to investigate transient phenomena. Second, the complicated geometry of these devices, different kinds of boundary conditions and uncertain values of material parameters make that even static cases are difficult to solve.

The authors who consider dynamical models usually concentrate on initial heating (temperature rise during the first current pulse) of the laser inside the resonator (Nakwaski (1983b)) or at the mirrors (Nakwaski (1985; 1990)). The papers mentioned above developed analytical solutions of time-dependent heat conduction equation using sophisticated mathematical methods, like for example Green function formalism or Kirchhoff transformation. Numerical approach to this class of problems appeared much later. As an example see Puchert et al. (2000), where laser array was investigated. It is noteworthy that the heat source function was obtained by a rate equation model. Remarkable agreement with experimental temperature values showed the importance of the concept of distributed heat sources. The author has theoretically investigated the dynamical thermal behaviour of

Layer	thickness $[\mu m]$	$\lambda[\mathrm{W/(mK)}]$	$c_h[\mathrm{J/(kgK)}]$	$\rho[\mathrm{kg/m^3}]$	heat source
substrate	100	44	327	5318	yes - equation (11)
$Al_{0.6}Ga_{0.4}As$ (n-cladding)	1.5	11.4	402	4384	no
$Al_{0.4}Ga_{0.6}As$ (waveguide)	0.35	11.1	378	4696	yes - equation (11)
active layer	0.007	44	327	5318	yes - equation (9)
$Al_{0.4}Ga_{0.6}As$ (waveguide)	0.59	11.1	378	4696	yes - equation (11)
$Al_{0.6}Ga_{0.4}As$ (p-cladding)	1.5	11.4	402	4384	yes - equation (11)
GaAs (cap)	0.2	44	327	5318	no
p-contact	1	318	128	19300	no
In (solder)	1	82	230	7310	no

Table 3. Transverse structure of the investigated laser array.

p-down mounted 25-emitter laser array. Temperature profiles during first 10 pulses have been calculated (Fig. 12 and 13). The transverse structure of the device, material parameters and the distribution of heat sources are presented in Table 3. The time-dependent heat conduction equation

$$\rho(x,y,z)c_h(x,y,z)\frac{\partial T}{\partial t} = \nabla(\lambda(x,y,z)\nabla T) + g(x,y,z,t), \tag{18}$$

has been solved numerically.[6] The following boundary and initial conditions have been assumed:

— constant temperature $T = 300K$ at the heat spreader-heat sink interface;[7]
— convective cooling of the top surface ($\alpha = 35 * 10^3 WK^{-1}m^{-2}$);
— all side walls (including mirrors) thermally insulated;
— $T(x,y,z,t=0) = 300K$.

Note that the considered laser array has been driven by rectangular pulses of period 3.33 ms and 50% duty cycle, while the carrier lifetime is of the order of several nanoseconds. Thus, the electron response for the applied voltage can be regarded as immediate[8] and equation (8) can be transformed to the time-dependent function in the following way:

$$g(x,y,z,t) = [g_a(x,y,z) + g_J(x,y,z)]\Theta(t), \tag{19}$$

[6] Calculations have been done by Zenon Gniazdowski using the commercial software CFDRC (http://www.cfdrc.com/).
[7] To simplify the problem, the ideal heat sink $\lambda = \infty$ has been assumed.
[8] This statement is common for all standard edge-emitting devices.

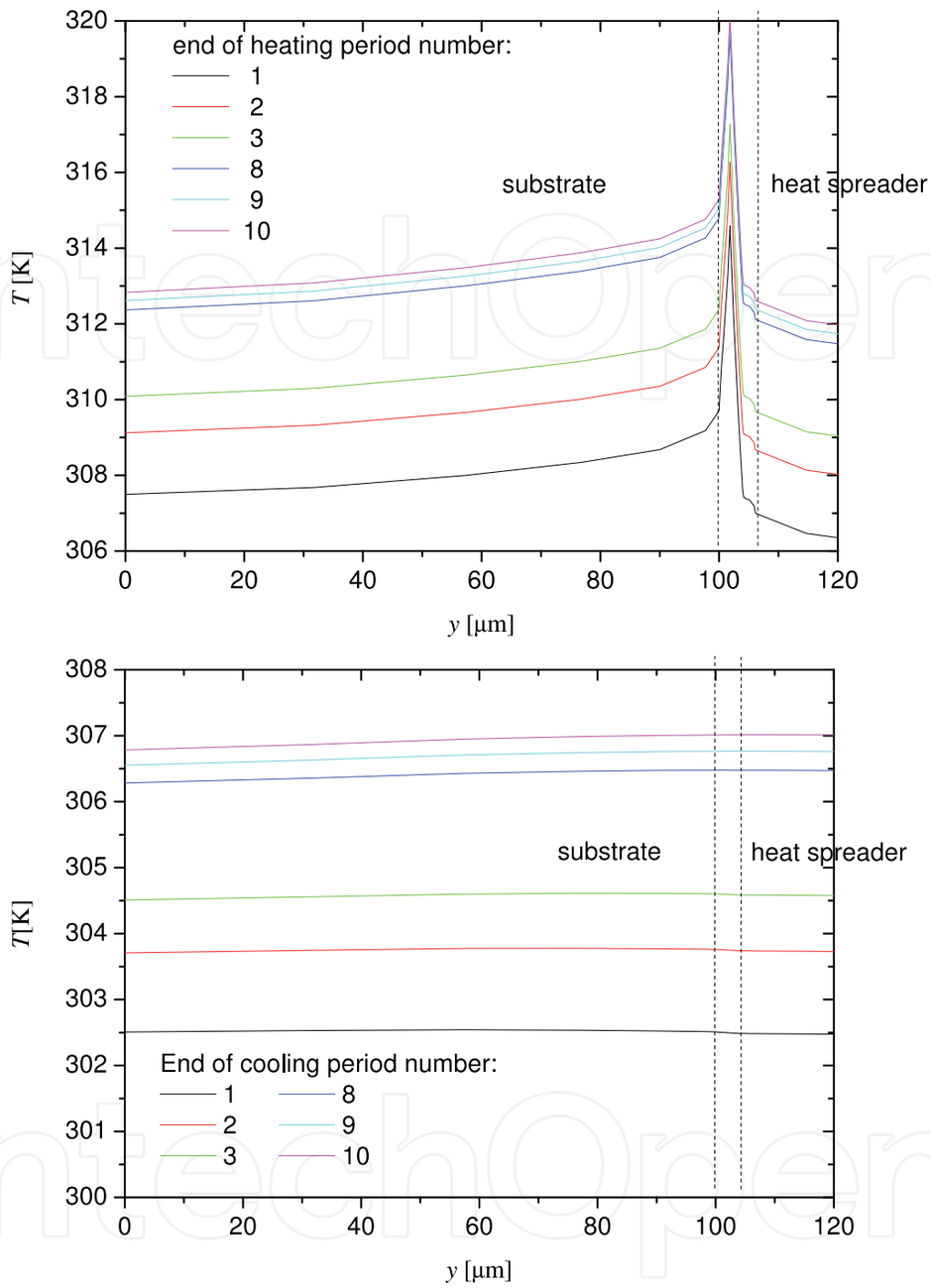

Fig. 13. Transverse temperature profiles at the front facet of the central emitter. Dashed vertical lines indicate the edges of heat spreader and substrate.

where $\Theta(t) = 1$ or 0 exactly reproduces the driving current changes.

7. Heat flow in a quantum cascade laser

Quantum-cascade lasers are semiconductor devices exploiting superlattices as active layers. In numerous experiments, it has been shown that the thermal conductivity λ of a superlattice

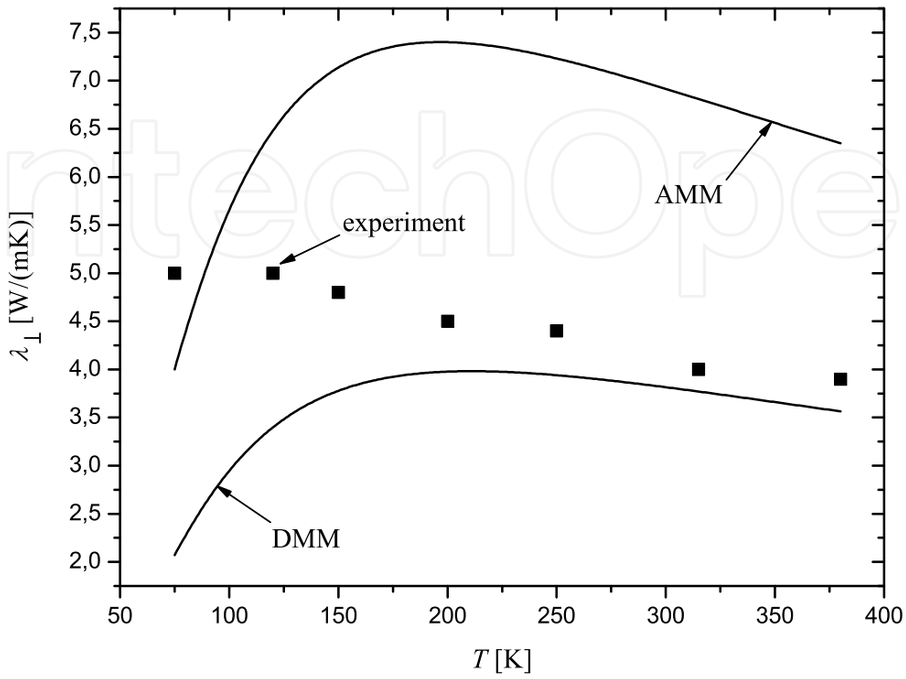

Fig. 14. Calculated cross-plane thermal conductivity for the active region of THz QCL (Szymański (2011)). Square symbols show the values measured by Vitiello et al. (2008).

is significantly reduced (Capinski et al. (1999); Cahill et al. (2003); Huxtable et al. (2002)). Particularly, the cross-plane value $\lambda_\perp$ may be even order-of-magnitude smaller than than the value for constituent bulk materials. The phenomenon is a serious problem for QCLs, since they are electrically pumped by driving voltages over 10 V and current densities over 10 kA/cm^2. Such a high injection power densities lead to intensive heat generation inside the devices. To make things worse, the main heat sources are located in the active layer, where the density of interfaces is the highest and—in consequence—the heat removal is obstructed. Thermal management in this case seems to be the key problem in design of the improved devices.

Theoretical description of heat flow across SL's is a really hard task. The crucial point is finding the relation between phonon mean free path Λ and SL period D Yang & Chen (2003). In case $\Lambda > D$, both wave- and particle-like phonon behaviour is observed. The thermal conductivity is calculated through the modified phonon dispersion relation obtained from the equation of motion of atoms in the crystal lattice (see for example Tamura et al. (1999)). In case $\Lambda < D$, phonons behave like particles. The thermal conductivity is usually calculated using the Boltzmann transport equation with boundary conditions involving diffuse scattering.

Unfortunately, using the described methods in the thermal model of QCL's is questionable. They are very complicated on the one hand and often do not provide satisfactionary results on the other. The comprehensive comparison of theoretical predictions with experiments for

nanoscale heat transport can be found in Table II in Cahill et al. (2003). This topic was also widely discussed by Gesikowska & Nakwaski (2008). In addition, the investigations in this field usually deal with bilayer SL's, while one period of QCL active layer consists of dozen or so layers of order-of-magnitude thickness differences.

Consequently, present-day mathematical models of heat flow in QCLs resemble those created for standard edge emitting lasers: they are based on heat conduction equation, isothermal condition at the bottom of the structure and convective cooling of the top and side walls are assumed. QCL's as unipolar devices are not affected by surface recombination. Their mirrors may be hotter than the inner part of resonator only due to bonding imperfections (see 8.4). Colour maps showing temperature in the QCL cross-section and illustrating fractions of heat flowing through particular surfaces can be found in Lee et al. (2009) and Lops et al. (2006). In those approaches, the SL's were replaced by equivalent layers described by anisotropic values of thermal conductivity $\lambda_{\perp}$ and $\lambda_{\parallel}$ arbitrarily reduced (Lee et al. (2009)) or treated as fitting parameters (Lops et al. (2006)).

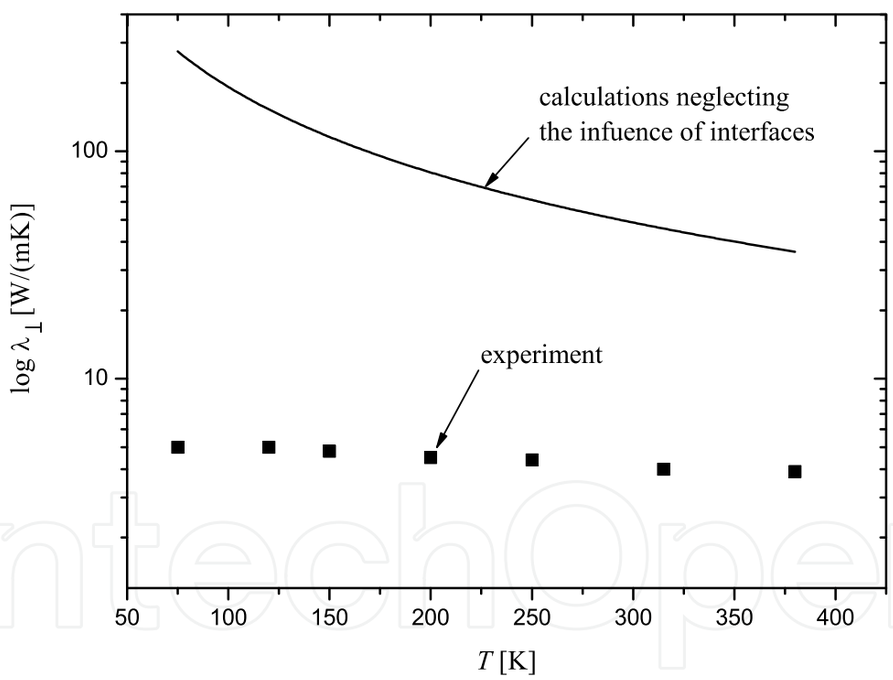

Fig. 15. Illustration of significant discrepancy between values of $\lambda_{\perp}$ measured by Vitiello et al. (2008) and calculated according to equation (20), which neglects the influence of interfaces (Szymański (2011)).

Proposing a relatively simple method of assessing the thermal conductivity of QCL active region has been a subject of several works. A very interesting idea was mentioned by Zhu et al. (2006) and developed by Szymański (2011). The method will be briefly described below.

The thermal conductivity of a multilayered structure can be approximated according to the rule of mixtures Samvedi & Tomar (2009); Zhou et al. (2007):

$$\lambda^{-1} = \sum_n f_n \lambda_n^{-1}, \tag{20}$$

where f_n and λ_n are the volume fraction and bulk thermal conductivity of the n-th material. However, in case of high density of interfaces, the approach (20) is inaccurate because of the following reason. The interface between materials of different thermal and mechanical properties obstructs the heat flow, introducing so called 'Kapitza resistance' or thermal boundary resistance (TBR) Swartz & Pohl (1989). The phenomenon can be described by two phonon scattering models, namely the acoustic mismatch model (AMM) and the diffuse mismatch model (DMM). Input data are limited to such basic material parameters like Debye temperature, density or acoustic wave speed. Thus, the thermal conductivity of the QCL active region can be calculated as a sum of weighted average of constituent bulk materials reduced by averaged TBR multiplied by the number of interfaces:

$$\lambda_\perp^{-1} = \frac{d_1}{d_1 + d_2} r_1 + \frac{d_2}{d_1 + d_2} r_2 + \frac{n_i}{d_1 + d_2} r_{\mathrm{Bd}}^{(\mathrm{av})}, \tag{21}$$

where TBR has been averaged with respect to the direction of the heat flow

$$r_{\mathrm{Bd}}^{(\mathrm{av})} = \frac{r_{\mathrm{Bd}}(1 \to 2) + r_{\mathrm{Bd}}(2 \to 1)}{2}. \tag{22}$$

The detailed prescription on how to calculate $r_{\mathrm{Bd}}^{(\mathrm{av})}$ can be found in Szymański (2011).
The model based on equations (21) and (22) was positively tested on bilayer $Si_{0.84}Ge_{0.16}/Si_{0.74}Ge_{0.26}$ SL's investigated experimentally by Huxtable et al. (2002). Then, $GaAs/Al_{0.15}Ga_{0.85}As$ THz QCL was considered. Results of calculations exhibit good convergence with measurements presented by Vitiello et al. (2008) as shown in Fig. 14. On the contrary, values of $\lambda_\perp$ calculated according to equation (20), neglecting the influence of interfaces, show significant discrepancy with the measured ones (Fig. 15).

8. Summary

Main conclusions or hints dealing with thermal models of edge-emitting lasers will be aggregated in the form of the following paragraphs.

8.1 Differential equations

A classification of thermal models is presented in Table 4. Basic thermal behaviour of an edge-emitting laser can be described according to Approach 1. It is assumed that the heat power is generated uniformly in selected regions: mainly in active layer and, in minor degree, in highly resistive layers. Considering the laser cross-section parallel to mirrors' surfaces and reducing the dimensionality of the heat conduction equation to 2 is fully justified. For calculating the temperature in the entire device (including the vicinity of mirrors) Approach 2 should be used. The main heat sources may be determined as functions of carrier concentration calculated from the diffusion equation. It is recommended to use three-dimensional heat conduction equation. The diffusion equation can be solved in the

Approach	Equations(s)	Calculated T		Application	Example references
		inside the resonator	in the vicinity of mirrors		
1	HC	yes	near-threshold regime	basic thermal behaviour of a laser	Joyce & Dixon (1975), Puchert et al. (1997), Szymański et al. (2007)
2	HC+D	yes	low-power operation	thermal behaviour of a laser including the vicinity of mirrors	Chen & Tien (1993), Mukherjee & McInerney (2007)
3	HC+D+PR	yes	high-power operation	facet temperature reduction	Romo et al. (2003)

Table 4. A classification of thermal models. Abbreviations: HC-heat conduction, D-diffusion, PR -photon rate.

plane of junction (2 dimensions) or reduced to the axial direction (1 dimension). Approach 3 is the most advanced one. It is based on 4 differential equations, which should be solved in self-consisted loop (see Fig. 9). Approach 3 is suitable for standard devices as well as for lasers with modified close-to-facet regions.

8.2 Boundary conditions

The following list presents typical boundary conditions (see for example Joyce & Dixon (1975), Puchert et al. (1997), Szymański et al. (2007)):

— isothermal condition at the bottom of the device,

— thermally insulated side walls,

— convectively cooled or thermally insulated (which is the case of zero convection coefficient) upper surface.

In Szymański (2007), it was shown that assuming isothermal condition at the upper surface is also correct and reveals better convergence with experiment.
Specifying the bottom of the device may be troublesome. Considering the heat flow in the chip only, i.e. assuming the ideal heat sink, leads to significant errors (Szymański et al. (2007)). On the other hand taking into account the whole assembly (chip, heat spreader and heat sink) is difficult. In the case of analytical approach, it significantly complicates the geometry of the thermal scheme. In order to avoid that tricky modifications of thermal scheme (like in Szymański et al. (2007)) have to be introduced. In case of numerical approach, using non-uniform mesh is absolutely necessary (see for example Puchert et al. (2000)).
In Ziegler et al. (2006), an actively cooled device was investigated. In that case a very strong convection ($\alpha = 40 * 10^4 W/(mK)$) at the bottom surface was assumed in calculations.

8.3 Calculation methods

Numerous works dealing with thermal modelling of edge-emitting lasers use analytical approaches. Some of them exploit highly sophisticated mathematical methods. For example,

Kirchhoff transformation (see Nakwaski (1980)) underlied further pioneering theoretical studies on the COD process by Nakwaski (1985) and Nakwaski (1990), where solutions of the three-dimensional time-dependent heat conduction equation were found using the Green function formalism. Conformal mapping has been used by Laikhtman et al. (2004) and Laikhtman et al. (2005) for thermal optimisation of high power diode laser bars. Relatively simple separation-of-variables approach was used by Joyce & Dixon (1975) and developed in many further works (see for example Bärwolff et al. (1995) or works by the author of this chapter).

Analytical models often play a very helpful role in fundamental understanding of the device operation. Some people appreciate their beauty. However, one should keep in mind that edge-emitting devices are frequently more complicated. This statement deals with the internal chip structure as well as packaging details. Analytical solutions, which can be found in widely-known textbooks (see for example Carslaw & Jaeger (1959)), are usually developed for regular figures like rectangular or cylindrical rods made of homogeneous materials. Small deviation from the considered geometry often leads to substantial changes in the solution. In addition, as far as solving single heat conduction equation in some cases may be relatively easy, including other equations enormously complicates the problem. Recent development of simulation software based on Finite Element Method creates the temptation to relay on numerical methods. In this chapter, the commercial software has been used for computing dynamical temperature profiles (Fig. 12 and 13)[9] and carrier concentration profiles (Fig. 7 and 8).[10] Commercial software was also used in many works, see for example Mukherjee & McInerney (2007); Puchert et al. (2000); Romo et al. (2003). In Ziegler et al. (2006; 2008), a self-made software based on FEM provided results highly convergent with sophisticated thermal measurements of high-power diode lasers. Thus, nowadays numerical methods seem to be more appropriate for thermal analysis of modern edge-emitting devices. However, one may expect that analytical models will not dissolve and remain as helpful tools for crude estimations, verifications of numerical results or fundamental understanding of particular phenomena.

8.4 Limitations

While using any kind of model, one should be prepared for unavoidable inaccuracies of the temperature calculations caused by factors characteristic for individual devices, which elude qualitative assessment. The paragraphs below briefly describe each factor.

Real solder layers may contain a number of voids, such as inclusions of air, clean-up agents or fluxes. Fig. 12 in Bärwolff et al. (1995) shows that small voids in the solder only slightly obstruct the heat removal from the laser chip to the heat sink unless their concentration is very high. In turn, the influence of one large void is much bigger: the device thermal resistance grows nearly linearly with respect to void size.

The laser chip may not adhere to the heat sink entirely due to two reasons: the metallization may not extend exactly to the laser facets or the chip can be inaccurately bonded (it can extend over the heat sink edge). In Lynch (1980), it was shown that such an overhang may contribute to order of magnitude increase of the device thermal resistance.

[9] CFDRC software (http://www.cfdrc.com/) used used by Zenon Gniazdowski.
[10] FlexPDE software (http://www.pdesolutions.com/) used by Michal Szymański.

In Pipe & Ram (2003) it was shown that convective cooling of the top and side walls plays a significant role. Unfortunately, determining of convective coefficient is difficult. The values found in the literature differ by 3 order-of-magnitudes (see Szymański (2007)).
Surface recombination, one of the two main mirror heating mechanisms, strongly depends on facet passivation. The significant influence of this phenomenon on mirror temperature was shown in Diehl (2000). It is noteworthy that the authors considered values v_{sur} of one order-of-magnitude discrepancy.[11]
Modern devices often consist of multi-compound semiconductors of unknown thermal properties. In such cases, one has to rely on approximate expressions determining particular parameter upon parameters of constituent materials (see for example Nakwaski (1988)).

8.5 Quantum cascade lasers

Present-day mathematical models of heat flow in QCL resemble those created for standard edge emitting lasers: they are based on heat conduction equation, isothermal condition at the bottom of the structure and convective cooling of the top and side walls are assumed. The SL's, which are the QCLs' active regions, are replaced by equivalent layers described by anisotropic values of thermal conductivity $\lambda_{\perp}$ and $\lambda_{\parallel}$ arbitrarily reduced (Lee et al. (2009)), treated as fitting parameters (Lops et al. (2006)) or their parameters are assessed by models considering microscale heat transport (Szymański (2011)).

9. References

Bärwolff A., Puchert R., Enders P., Menzel U. and Ackermann D. (1995) Analysis of thermal behaviour of high power semiconductor laser arrays by means of the finite element method (FEM), *J. Thermal Analysis*, Vol. 45, No. 3, (September 1995) 417-436.

Bugajski M., Piwonski T., Wawer D., Ochalski T., Deichsel E., Unger P., and Corbett B. (2006) Thermoreflectance study of facet heating in semiconductor lasers, *Materials Science in Semiconductor Processing* Vol. 9, No. 1-3, (February-June 2006) 188-197.

Capinski W S, Maris H J, Ruf T, Cardona M, Ploog K and Katzer D S (1999) Thermal-conductivity measurements of GaAs/AlAs superlattices using a picosecond optical pump-and-probe technique, *Phys. Rev. B*, Vol. 59, No. 12, (March 1999) 8105-8113.

Carslaw H. S. and Jaeger J. C. (1959) *Conduction of heat in solids*, Oxford University Press, ISBN, Oxford.

Cahill D. G., Ford W. K., Goodson K. E., Mahan G. D., Majumdar A., Maris H. J., Merlin R. and Phillpot S. R. (2003) Nanoscale thermal transport, *J. Appl. Phys.*, Vol. 93, No. 2, (January 2003) 793-818.

Chen G. and Tien C. L. (1993) Facet heating of quantum well lasers, *J. Appl. Phys.*, Vol. 74, No. 4, (August 1993) 2167-2174.

Diehl R. (2000) *High-Power Diode Lasers. Fundamentals, Technology, Applications*, Springer, ISBN, Berlin.

[11] Surface recombination does not deal with QCL's as they are unipolar devices. In turn, inaccuracies related to assessing $\lambda_{\perp}$ and $\lambda_{\parallel}$ may occur.

Gesikowska E. and Nakwaski W. (2008) An impact of multi-layered structures of modern optoelectronic devices on their thermal properties, *Opt. Quantum Electron.*, Vol. 40, No. 2-4, (August 2008) 205-216.

Huxtable S. T., Abramson A. R., Chang-Lin T., and Majumdar A. (2002) Thermal conductivity of Si/SiGe and SiGe/SiGe superlattices *Appl. Phys. Lett.* Vol. 80, No. 10, (March 2002) 1737-1739.

Joyce W. B. & Dixon R. (1975). Thermal resistance of heterostructure lasers, *J. Appl. Phys.*, Vol. 46, No. 2, (February 1975) 855-862.

Laikhtman B., Gourevitch A., Donetsky D., Westerfeld D. and Belenky G. (2004) Current spread and overheating of high power laser bars, *J. Appl. Phys.*, Vol. 95, No. 8, (April 2004) 3880-3889.

Laikhtman B., Gourevitch A., Westerfeld D., Donetsky D. and Belenky G., (2005) Thermal resistance and optimal fill factor of a high power diode laser bar, *Semicond. Sci. Technol.*, Vol. 20, No. 10, (October 2005) 1087-1095.

Lee H. K., Chung K. S., Yu J. S. and Razeghi M. (2009) Thermal analysis of buried heterostructure quantum cascade lasers for long-wave-length infrared emission using 2D anisotropic, heat-dissipation model, *Phys. Status Solidi A*, Vol. 206, No. 2, (February 2009) 356-362.

Lops A., Spagnolo V. and Scamarcio G. (2006) Thermal modelling of GaInAs/AlInAs quantum cascade lasers, *J. Appl. Phys.*, Vol. 100, No. 4, (August 2006) 043109-1-043109-5.

Lynch Jr. R. T. (1980) Effect of inhomogeneous bonding on output of injection lasers, *Appl. Phys. Lett.*, Vol. 36, No. 7, (April 1980) 505-506.

Manning J. S. (1981) Thermal impedance of diode lasers: Comparison of experimental methods and a theoretical model, *J. Appl. Phys.*, Vol. 52, No. 5, (May 1981) 3179-3184.

Mukherjee J. and McInerney J. G. (2007) Electro-thermal Analysis of CW High-Power Broad-Area Laser Diodes: A Comparison Between 2-D and 3-D Modelling, *IEEE J. Sel. Topics in Quantum Electron.* , Vol. 13, No. 5, (September/October 2007) 1180-1187.

Nakwaski W. (1979) Spontaneous radiation transfer in heterojunction laser diodes, *Sov. J. Quantum Electron.*, Vol. 9, No. 12, (December 1979) 1544-1546.

Nakwaski W. (1980) An application of Kirchhoff transformation to solving the nonlinear thermal conduction equation for a laser diode, *Optica Applicata*, Vol. 10, No. 3, (?? 1980) 281-283.

Nakwaski W. (1983) Static thermal properties of broad-contact double heterostructure GaAs-(AlGa)As laser diodes, *Opt. Quantum Electron.*, Vol. 15, No. 6, (November 1983) 513-527.

Nakwaski W. (1983) Dynamical thermal properties of broad-contact double heterostructure GaAs-(AlGa)As laser diodes, *Opt. Quantum Electron.*, Vol. 15, No. 4, (July 1983) 313-324.

Nakwaski W. (1985) Thermal analysis of the catastrophic mirror damage in laser diodes, *J. Appl. Phys.*, Vol. 57, No. 7, (April 1985) 2424-2430.

Nakwaski W. (1988) Thermal conductivity of binary, ternary and quaternary III-V compounds, *J. Appl. Phys.*, Vol. 64, No. 1, (July 1988) 159-166.

Nakwaski W. (1990) Thermal model of the catastrophic degradation of high-power stripe-geometry GaAs-(AlGa)As double-heterostructure diode-lasers, *J. Appl. Phys.*, Vol. 67, No. 4, (February 1990) 1659-1668.

Pierscińska D., Piersciński K., Kozlowska A., Malag A., Jasik A. and Poprawe R. (2007) Facet heating mechanisms in high power semiconductor lasers investigated by spatially resolved thermo-reflectance, *MIXDES*, ISBN, Ciechocinek, Poland, June 2007

Pipe K. P. and Ram R. J. (2003) Comprehensive Heat Exchange Model for a Semiconductor Laser Diode, *IEEE Photonic Technology Letters*, Vol. 15, No. 4, (April 2003) 504-506.

Piprek J. (2003) *Semiconductor optoelectronic devices. Introduction to physics and simulation*, Academic Press, ISBN 0125571909, Amsterdam.

Puchert R., Menzel U., Bärwolff A., Voß M. and Lier Ch. (1997) Influence of heat source distributions in GaAs/GaAlAs quantum-well high-power laser arrays on temperature profile and thermal resistance, *J. Thermal Analysis*, Vol. 48, No. 6, (June 1997) 1273-1282.

Puchert R., Bärwolff A., Voß M., Menzel U., Tomm J. W. and Luft J. (2000) Transient thermal behavior of high power diode laser arrays, *IEEE Components, Packaging, and Manufacturing Technology Part A* Vol. 23, No. 1, (January 2000) 95-100.

Rinner F., Rogg J., Kelemen M. T., Mikulla M., Weimann G., Tomm J. W., Thamm E. and Poprawe R. (2003) Facet temperature reduction by a current blocking layer at the front facets of high-power InGaAs/AlGaAs lasers, *J. Appl. Phys.*, Vol. 93, No. 3, (February 2003) 1848-1850

Romo G., Smy T., Walkey D. and Reid B. (2003) Modelling facet heating in ridge lasers, *Microelectronics Reliability*, Vol. 43, No. 1, (January 2003) 99-110.

Samvedi V. and Tomar V. (2009) The role of interface thermal boundary resistance in the overall thermal conductivity of Si-Ge multilayered structures, *Nanotechnology*, Vol. 20, No. 36, (September 2009) 365701.

Sarzała R. P. and Nakwaski W. (1990) An appreciation of usability of the finite element method for the thermal analysis of stripe-geometry diode lasers, *J. Thermal Analysis*, Vol. 36, No. 3, (May 1990) 1171-1189.

Sarzała R. P. and Nakwaski W. (1994) Finite-element thermal model for buried-heterostructure diode lasers, *Opt. Quantum Electron.* , Vol. 26, No. 2, (February 1994) 87-95.

Schatz R. and Bethea C. G. (1994) Steady state model for facet heating to thermal runaway in semiconductor lasers, *J. Appl. Phys.* , Vol. 76, No. 4, (August 1994) 2509-2521.

Swartz E. T. and Pohl R. O. (1989) Thermal boundary resistance *Rev. Mod. Phys.*, Vol. 61, No. 3, (July 1989) 605-668.

Szymański M., Kozlowska A., Malag A., and Szerling A. (2007) Two-dimensional model of heat flow in broad-area laser diode mounted to the non-ideal heat sink, *J. Phys. D: Appl. Phys.*, Vol. 40, No. 3, (February 2007) 924-929.

Szymański M. (2010) A new method for solving nonlinear carrier diffusion equation in axial direction of broad-area lasers, *Int. J. Num. Model.*, Vol. 23, No. 6, (November/December 2010) 492-502.

Szymański M. (2011) Calculation of the cross-plane thermal conductivity of a quantum cascade laser active region *J. Phys. D: Appl. Phys.*, Vol. 44, No. 8, (March 2011) 085101-1-085101-5.

Szymański M., Zbroszczyk M. and Mroziewicz B. (2004) The influence of different heat sources on temperature distributions in broad-area lasers *Proc. SPIE* Vol. 5582, (September 2004) 127-133.

Szymański M. (2007) Two-dimensional model of heat flow in broad-area laser diode: Discussion of the upper boundary condition *Microel. J.* Vol. 38, No. 6-7, (June-July 2007) 771-776.

Tamura S, Tanaka Y and Maris H J (1999) Phonon group velocity and thermal conduction in superlattices *Phys. Rev. B* , Vol. 60, No. 4, (July 1999) 2627-2630.

Vitiello M. S., Scamarcio G. and Spagnolo V. 2008 Temperature dependence of thermal conductivity and boundary resistance in THz quantum cascade lasers *IEEE J. Sel. Top. in Quantum Electron.*, Vol. 14, No. 2, (March/April 2008) 431-435 .

Watanabe M., Tani K., Takahashi K., Sasaki K., Nakatsu H., Hosoda M., Matsui S., Yamamoto O. and Yamamoto S. (1995) Fundamental-Transverse-Mode High-Power AlGaInP Laser Diode with Windows Grown on Facets, *IEEE J. Sel. Topics in Quantum Electron.*, Vol. 1, No. 2, (June 1995) 728-733.

Wawer D., Ochalski T.J., Piwoński T., Wójcik-Jedlińska A., Bugajski M., and Page H. (2005) Spatially resolved thermoreflectance study of facet temperature in quantum cascade lasers, *Phys. Stat. Solidi (a)* Vol. 202, No. 7, (May 2005) 1227-1232.

Yang B and Chen G (2003) Partially coherent phonon heat conduction in superlattices, *Phys. Rev. B*, Vol. 67, No. 19, (May 2003) 195311-1-195311-4.

Zhu Ch., Zhang Y., Li A. and Tian Z. 2006 Analysis of key parameters affecting the thermal behaviour and performance of quantum cascade lasers, *J. Appl. Phys.*, Vol. 100, No. 5, (September 2006) 053105-1-053105-6.

Zhou Y., Anglin B. and Strachan A. 2007 Phonon thermal conductivity in nanolaminated composite metals via molecular dynamics, *J. Chem. Phys.*, Vol. 127, No. 18, (November 2007) 184702-1-184702-11.

Ziegler M., Weik F., Tomm J.W., Elsaesser T., Nakwaski W., Sarzała R.P., Lorenzen D., Meusel J. and Kozlowska A. (2006) Transient thermal properties of high-power diode laser bars *Appl. Phys. Lett.* Vol. 89, No. 26, (December 2006) 263506-1-263506-3.

Ziegler M., Tomm J.W., Elsaesser T., Erbert G., Bugge F., Nakwaski W. and Sarzała R.P. (2008) Visualisation of heat flows in high-power diode lasers by lock-in thermography *Appl. Phys. Lett.* Vol. 92, No. 10, (March 2008) 103513-1-103513-3.

IntechOpen

Heat Transfer - Engineering Applications
Edited by Prof. Vyacheslav Vikhrenko

ISBN 978-953-307-361-3
Hard cover, 400 pages
Publisher InTech
Published online 22, December, 2011
Published in print edition December, 2011

Heat transfer is involved in numerous industrial technologies. This interdisciplinary book comprises 16 chapters dealing with combined action of heat transfer and concomitant processes. Five chapters of its first section discuss heat effects due to laser, ion and plasma-solid interaction. In eight chapters of the second section engineering applications of heat conduction equations to the curing reaction kinetics in manufacturing process, their combination with mass transport or ohmic and dielectric losses, heat conduction in metallic porous media and power cables are considered. Analysis of the safety of mine hoist under influence of heat produced by mechanical friction, heat transfer in boilers and internal combustion engine chambers, management for ultrahigh strength steel manufacturing are described in this section as well. Three chapters of the last third section are devoted to air cooling of electronic devices.

How to reference
In order to correctly reference this scholarly work, feel free to copy and paste the following:

Michał Szymanski (2011). Mathematical Models of Heat Flow in Edge-Emitting Semiconductor Lasers, Heat Transfer - Engineering Applications, Prof. Vyacheslav Vikhrenko (Ed.), ISBN: 978-953-307-361-3, InTech, Available from: http://www.intechopen.com/books/heat-transfer-engineering-applications/mathematical-models-of-heat-flow-in-edge-emitting-semiconductor-lasers

INTECH
open science | open minds

InTech Europe
University Campus STeP Ri
Slavka Krautzeka 83/A
51000 Rijeka, Croatia
Phone: +385 (51) 770 447
Fax: +385 (51) 686 166
www.intechopen.com

InTech China
Unit 405, Office Block, Hotel Equatorial Shanghai
No.65, Yan An Road (West), Shanghai, 200040, China
中国上海市延安西路65号上海国际贵都大饭店办公楼405单元
Phone: +86-21-62489820
Fax: +86-21-62489821

© 2011 The Author(s). Licensee IntechOpen. This is an open access article distributed under the terms of the Creative Commons Attribution 3.0 License, which permits unrestricted use, distribution, and reproduction in any medium, provided the original work is properly cited.

IntechOpen

IntechOpen